Journal of Orthopaedic Translation 29 (2021) 51–59

Contents lists available at ScienceDirect

Journal of Orthopaedic Translation

journal homepage: www.journals.elsevier.com/journal-of-orthopaedic-translation

3D ultrasound imaging provides reliable angle measurement with validity comparable to X-ray in patients with adolescent idiopathic scoliosis

Timothy Tin-Yan Lee [a], Kelly Ka-Lee Lai [a], Jack Chun-Yiu Cheng [b], René Marten Castelein [c], Tsz-Ping Lam [b], Yong-Ping Zheng [a,*]

[a] Department of Biomedical Engineering, The Hong Kong Polytechnic University, Hong Kong
[b] SH Ho Scoliosis Research Lab, Joint Scoliosis Research Center of the Chinese University of Hong Kong and Nanjing University, Department of Orthopaedics & Traumatology, The Chinese University of Hong Kong, Hong Kong
[c] Department of Orthopaedic Surgery, University Medical Center Utrecht, Utrecht, the Netherlands

ARTICLE INFO

Keywords:
Curve angles
Reliability
Validity
Scoliosis
Three-dimensional ultrasound imaging

ABSTRACT

Background & Objective: The application of ultrasound imaging for spine evaluation could minimize radiation exposure for patients with adolescence idiopathic scoliosis (AIS). A customized three-dimensional (3D) ultrasound imaging system has been demonstrated to provide reliable and valid coronal curvature measurements. However, these measurements were using the spinous processes as anatomical reference, leading to a predictable underestimation of the traditionally used Cobb angles. An alternative 3D ultrasound image reconstruction method was applied to create coronal images with more lateral features for angle measurement. The objective of this study was to test the reliability and the validity of this angle, the ultrasound curve angle (UCA), and compare the UCA with the Cobb angles on X-ray images of patients with AIS.

Materials and methods: This study was divided into: 1) Investigation of intra- and inter-reliability between two raters for measuring the UCA and two operators for acquiring ultrasound images; 2) Investigation of the validity between the radiographic Cobb angle and the UCA. Fifty patients and 164 patients with AIS, were included in the two stages, respectively. Patients underwent bi-planar X-ray and 3D ultrasound scanning on the same day. The proposed UCA was used to measure the coronal curvature from the ultrasound coronal images, which were formed using a newly customized volume projection imaging (VPI) method. The intra-rater/operator and inter-rater and operator reliability of the UCA were tested by intra-class correlation coefficient (ICC) (3,1) and (2,1), respectively. The validity of UCA measurements as compared to radiographic Cobb angles was tested by inter-method ICC (2,1), mean absolute difference (MAD), standard error of measurement (SEM), Pearson correlation coefficient and Bland–Altman statistics. The level of significance was set as 0.05.

Results: Excellent intra-rater and intra-operator (ICC (3,1)$\geq$0.973) and excellent inter-rater and inter-operator reliability (ICC (2,1)$\geq$0.925) for UCA measurement, with overall MAD and SEM no more than 3.5° and 1.7° were demonstrated for both main thoracic and (thoraco)lumbar curvatures. Very good correlations were observed between UCA and Cobb angle for main thoracic (R^2=0.893) and (thoraco)lumbar (R^2=0.884) curves. The mean (SD) measurements in terms of radiographic Cobb and UCA were 27.2 $\pm$ 11.6° and 26.3 $\pm$ 11.4° for main thoracic curves; and 26.2 $\pm$ 11.4° and 24.8 $\pm$ 9.7° for (thoraco)lumbar curve respectively. One hundred sixty-four subjects (33 male and 131 female subjects; 11–18 years of age, mean of 15.1 $\pm$ 1.9 years) were included for the validity session. Excellent inter-method variations (ICC (2,K) $\geq$0.933) with overall MAD and SEM no more than 3.0° and 1.5° were demonstrated for both main thoracic and (thoraco)lumbar curvatures. In addition, Bland–Altman plots demonstrated an acceptable agreement between ultrasound and radiographic Cobb measurements.

Conclusion: In this study, very good correlations and agreement were demonstrated between the ultrasound and X-ray measurements of the scoliotic curvature. Judging from the promising results of this study, patients with AIS

* Corresponding author. ST411, Department of Biomedical Engineering, The Hong Kong Polytechnic University, Hong Kong.
E-mail address: yongping.zheng@polyu.edu.hk (Y.-P. Zheng).

https://doi.org/10.1016/j.jot.2021.04.007
Received 22 July 2020; Received in revised form 13 April 2021; Accepted 15 April 2021

with different severity of curves can be evaluated and monitored by ultrasound imaging, reducing the usage of radiation during follow-ups. This method could also be used for scoliosis screening.
The Translational potential of this article: Ultrasound curve angle (UCA) obtained from 3D ultrasound imaging system can provide reliable and valid evaluation on coronal curvature for patients with AIS, without the need of radiation.

1. Introduction

Coronal Cobb angle measurement on upright posterior-anterior radiograph is the standard procedure to diagnose, monitor curve progression and assign treatments for patients with scoliosis in clinical practice. Adolescent idiopathic scoliosis (AIS) is the most prevalent structural spine disorder [1], however frequent exposure to radiation when monitoring scoliosis could increase the risk of cancer for these patients [2]. With the advancement of technology, low-dose bi-planar radiography, EOS system, was introduced and is increasingly being used for scoliosis evaluation and the images could be used for three-dimensional (3D) reconstruction [3]. However, relatively large difference in accuracy was found between the anterior and the posterior vertebral regions, since several anatomical landmarks on the posterior arch, such as the transverse and/or spinous processes, may be barely visible on the X-ray images, which causes reconstruction error that leads to results discrepancies [4]. However the effective dose of a X-ray received by a patients was still around 1 mSv [5], the radiation is cumulative as longitudinal follow-ups are generally required [6]. In addition, the operation and installation costs of the EOS system are relatively high, thus the cost effectiveness of this system is still controversial [7]. The need of a non-ionizing approach for spine assessments for patients with AIS thus leads to the emergence of various new imaging modalities for scoliosis, such as 3D ultrasound imaging, magnetic resonance imaging (MRI) and surface topographic methods. MRI is expensive too and is performed supine, while surface topography lacks standardization and only reflects the symmetry of the back surface but not the true spinal curvature [8].

Modern 3D ultrasound imaging is becoming more popular for assessing structural spine changes because of its non-ionizing nature, it is performed upright, and is inexpensive and user-friendly. Evaluation of spinal curvature and rotation using ultrasound has first been exploited by Suzuki et al. [9]. In more recent studies, different ultrasound landmarks have been identified and investigated for the possibility of using them for coronal spinal curvature evaluation. Spinous process angle (SPA), the angle formed between the lines drawn on the most tilted part of the spinous processes shadows, was used to evaluate coronal spine disorder of patients with AIS on the coronal ultrasound images in those studies, where the results were demonstrated to be reliable and valid compared with the radiographic Cobb [10–12]. Brink et al. further evaluated different measurement methods on ultrasound images to investigate the most appropriate way to measure curve severity in the main thoracic and (thoraco)lumbar region, where (thoraco)lumbar region specifies both thoracolumbar and lumbar curves [11]. The SPA has also been demonstrated to be reliable for investigating the effectiveness of orthotic treatment and coronal curvature asymmetry using other 3D ultrasound imaging system [13]. One limitation with SPA is that it underestimates the severity of the curve when compared to the traditional Cobb angle measurement [10,11]. The scaling factor between SPA and Cobb angles in these studies was not close to 1. Nevertheless, it has been previously reported that there was no statistically significant differences between the two parameters if a conversion using a scaling factor was applied [10–12]. The centre of laminae (COL) method had been used to evaluate coronal [14–16] and sagittal [17,18] spinal curvature on spine phantoms and patients with AIS. Although high intra- and inter-rater reliability and good correlation and agreement with Cobb angle were achieved for coronal angles using COL method, most of the curves involved were moderate and the total time required for coronal image construction, identification of landmarks and angle measurements was relatively long, approximately 3 min [16]. Furthermore, transverse processes angle has also been used to evaluate coronal curvatures on spine phantom [18] and human subjects [19], and demonstrated to correlate closely with Cobb angle. However, the practical usability of the system has yet to be confirmed for the former study and the visualization of the lateral features on the ultrasound images were not optimized for measurement for the latter study.

Although all the above studies demonstrated the feasibility of using ultrasound to assess coronal curvature for patients with AIS, they had their limitations. The sample sizes of ultrasound studies using bilateral features such as transverse processes or laminae to validate coronal ultrasound measurement were relatively small, from about 20 to 49 subjects. Thus the objective of this study was to evaluate the reliability and validity of a new measurement parameter, the ultrasound curve angle (UCA), on coronal curvature measurement on AIS spine, in comparison with the radiographic Cobb angle. Since the UCA used in this study has been applied to a relative larger group of patients with AIS with a wider range of curves compared to previous studies, the results would demonstrate that the UCA is a reliable ultrasound parameter.

2. Materials and methods

2.1. Subjects

Patients diagnosed with AIS within the age of 10–18, without metallic implants and body mass index (BMI) no more than 25.0 kg/m^2 were included in this study. All patients with AIS were recruited in the Department of Orthopaedics and Traumatology of The Chinese University of Hong Kong. All the patients were screened and diagnosed as AIS by a medical doctor in the orthopedics department who has over 15 years of experiences in reading radiographs of patients with scoliosis. The study received human subject ethical approvals from both The Hong Kong Polytechnic University and The Chinese University of Hong Kong. Informed consent was obtained from all patients. Patients were requested to receive both ultrasound scanning and X-ray imaging on the same day. For patients with braces, they were required to remove their braces 48 h prior to X-ray imaging.

2.2. 3D ultrasound imaging system and coronal image generation

The customized 3D ultrasound imaging system (Fig. 1a) and EOS® system (EOS imaging, Paris, France) were used for ultrasound and X-ray scanning, respectively. The ultrasound imaging system mainly consists of a linear ultrasound probe (central frequency of 7.5 MHz and 7.5 cm width) with an electromagnetic spatial sensor attached to it to detect the corresponding position and orientation of the probe. The patients received ultrasound scanning in a natural standing posture with arms resting by their side. The following procedures were performed prior to scanning: 1) Application of ultrasound gel to the back of the patients; 2) Defining the scanning range by identifying the level of T1 and L5 through observing the B-mode images; 3) Fine tuning of the ultrasound images by adjusting the time gain compensation control and brightness of the B-mode images. In addition, the system consists of chest and hip boards with supporters to minimize the motion of the patients caused by the sliding of the probe during scanning (Fig. 1b). The shoulder and hip supports were adjusted to support the patients without altering their natural standing postures. During scanning, the probe was manually

moved upwards from an area below L5 to above T1 (Fig. 1c). Subjects were allowed to breathe normally during the scanning procedure. According to our observation, the breathing does not affect the coronal curvature of spine. The average scanning time of a patient was around 30–40 s. Detailed specification of the 3D ultrasound imaging system and the testing protocol on human subjects had been reported in previous studies [10,18]. EOS® is a bi-planar X-ray imaging system which simultaneously provides upright coronal and sagittal radiographic images with low radiation dosage [3,20]. Subjects were required to stand naturally with extended hips and knees and with hands on a support about 1.7m from ground level.

After scanning, the collected B-mode images were merged into a 3D image based on the corresponding spatial information recorded and used for 3D ultrasound volume reconstruction. In previous studies, coronal ultrasound images were formed using volume projection imaging (VPI) method, which obtains an averaged intensity of all voxels in the ultrasound volume within a selected depth of approximately 10 mm from the skin surface along the anteroposterior direction, for coronal SPA measurement [10–12,21]. However, the proposed UCA method required the visualization of the lateral features to assess the coronal curvatures. As the previous VPI method utilized the back surface of the subject as the cutting plane for coronal image projection, it would not be the optimal because the lumbar vertebrae features were further away from the skin compared to those in the thoracic regions (Fig. 2a). Therefore, an alternative VPI method, which used a depth profile depending on the skin-to-laminae distances extracted from the sagittal ultrasound images of 40 patients with AIS of different severity, was adopted in this study for generating the coronal ultrasound images (Fig. 2b). To further cope with individual difference of depth profile for image projection, 9 VPI images were formed with different depths based on the representative depth profile for all subjects. In order to choose the most optimal layer for UCA measurement, the VPI image which exhibits most visible lateral features, especially in the most tilted regions for facilitating the UCA measurements, was selected by two raters who were responsible for measuring the ultrasound images. Both raters should agree with the selected images as the most optimal one. Fig. 3a and b illustrated the coronal ultrasound images formed from the alternative VPI method used in this study and the original VPI method used in a previous study from a patient with AIS.

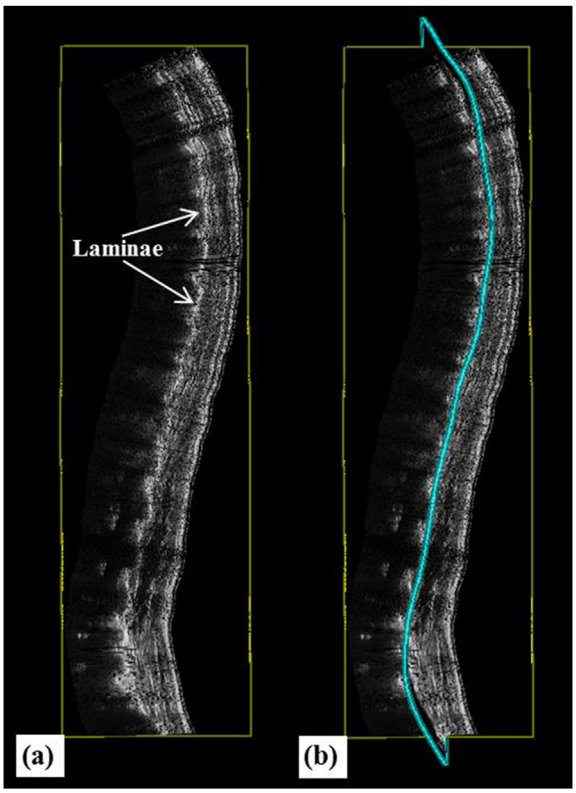

Figure 2. Diagram illustrating the (a) ultrasonic sagittal profile of the spine with vertebrae features such as laminae (arrow); (b) the representative depth profile (between vertebrae bony structure and skin as reference) in blue colour used for volume projection imaging to generate the alternative coronal ultrasound images in this study.

2.3. Angle measurements and study design

The raters were required to first manually identify the vertebrae levels and the transverse processes and laminae–articular processes shadows on the coronal ultrasound images to acquire the UCA. Prior to UCA measurement, evaluators would first have to locate proper points for

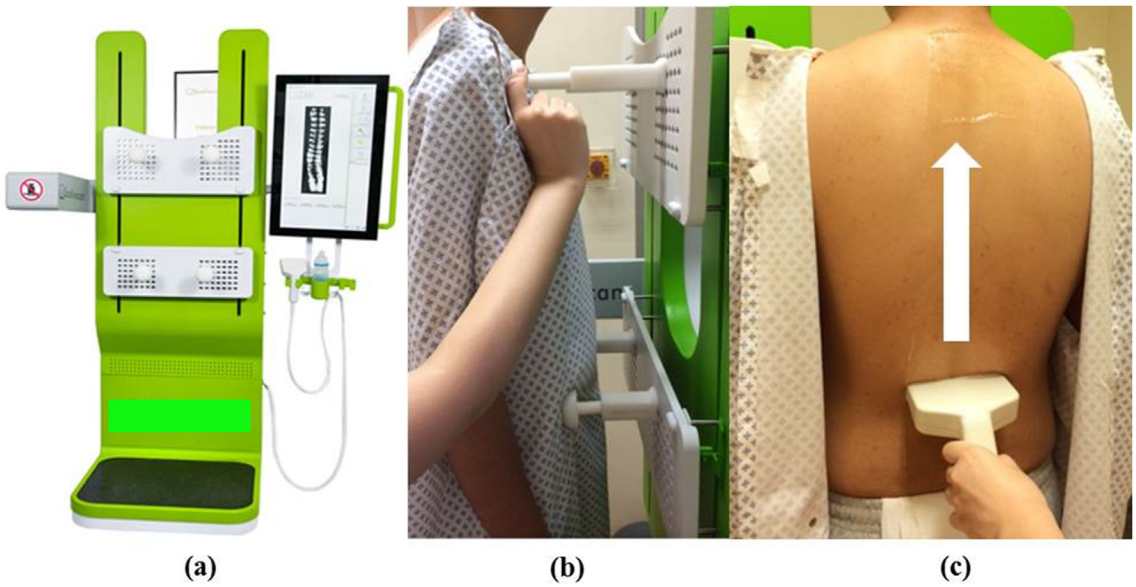

Figure 1. Diagram illustrating (a) The 3D ultrasound imaging system used for ultrasound scanning; (b) The adjustment of the supporters of the chest and hip boards before scanning; and (c) The upward sliding of the ultrasound probe to conduct the scanning.

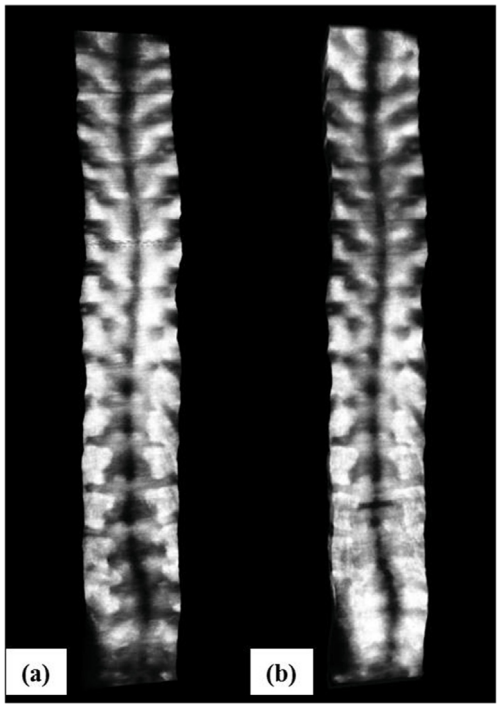

Figure 3. Diagram illustrating the (a) Coronal ultrasound image formed using skin surface as reference for VPI; (b) Coronal ultrasound image formed using the depth between vertebrae bony structure and skin as reference for VPI.

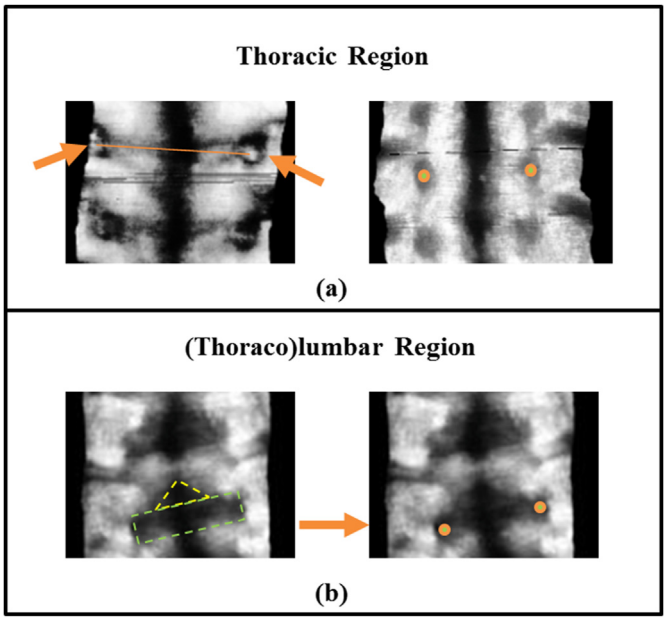

Figure 4. Diagrams illustrating how points for line placements were assigned to acquire UCA: a) For thoracic region, if a white dot, which corresponded to the echo of a transverse process, could be seen, the center of the white dot will be used to place the point (left); If no white dot could be observed, the centre of the black region, which corresponded to the shadow of a transverse process, will be used to place the point (right); b) For (thoraco)lumbar region, the lump shadow would be considered as a combination of a triangle (yellow dotted line) and a rectangle (green dotted line) (left). Dots will be placed at locations proximal to the centre of the bilateral sides of the rectangle (right). UCA: Ultrasound Curve Angle.

line placement on the ultrasound images. For thoracic region, the echoes or the shadows of the transverse processes would be first located (Fig. 4a), which generally appeared bilaterally between the shadows of the medial spinous process and the bilateral ribs and appeared in rounded shape, starting from the T12 level. A couple of lumps which appeared below T12 in the (thoraco)lumbar regions were formed by the combined shadows of the partial bilateral inferior articular processes, laminae and the superior articular processes of the inferior vertebrae (Fig. 4b). For instance, the first lump is formed by the T12 bilateral inferior articular processes, laminae and the L1 superior articular processes, the second lump is formed by the L1 bilateral inferior articular processes, laminae and the L2 superior articular processes and so on. Although the bilateral transverse processes could also be viewed in some occasion, they were not always observable or within the scanning range of the ultrasound, these landmarks were not considered for angle measurement in this study. The vertebrae structure selected for line drawing depended on the location of the uppermost and lowermost tilted region of the curve. The pair of T12 ribs, generally the last pair of ribs which appears from the bottom of the ultrasound image, was essential for classifying the vertebrae levels. For the most tilted region on T12 or above, line was drawn though the centre of the bilateral transverse processes shadows (Fig. 4a). For the most tilted region appearing below T12 level, the line was drawn though the centre of the widest bilateral part of the lump, which were formed mostly by the bilateral superior articular processes shadows (Fig. 4b). Afterwards, UCA were computed using the most tilted lines in the main thoracic and (thoraco)lumbar (Fig. 5a). For ultrasound images, curves were classified as main thoracic if the apex was located within T6 to T11/T12 transverse processes shadows or as (thoraco)lumbar if the apex was located below T11/T12

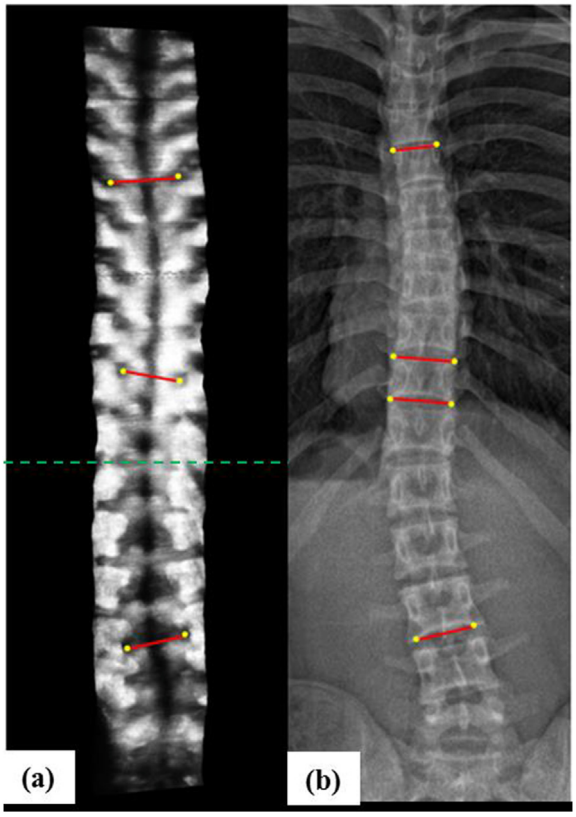

Figure 5. Diagram illustrating the (a) UCA measured on coronal ultrasound image and (b) Cobb angle measured on coronal X-ray images. The pair of T12 ribs was first identified to distinguish the rest of the vertebrae level (green dashed line). For cases with the most tilted vertebrae on T12 or above, line was placed though the centre of the bilateral transverse processes echoes or shadows, whereas for cases with the most tilted vertebrae below T12, the line was drawn though the centre of the bilateral superior articular processes shadows, which composed of the widest bilateral part of the lump.

transverse processes shadows. For X-ray images, Cobb angles were measured by the angle formed between the most tilted upper endplate the lower endplate on coronal X-ray images (Fig. 5b). Curves were classified as main thoracic if the apex was located within T6 to T11/T12 intervertebral disc or as (thoraco)lumbar if the apex was located below T11/T12 intervertebral disc, according to the SRS criteria. Both ultrasound and X-ray images measurements were performed on RadiAnt DICOM Viewer (Medixant, Poland). A medical doctor with 15 years of experiences in reading radiographs of patients with scoliosis was responsible for the coronal X-ray measurement, whereas two other raters who had at least 5 years of experience on scoliosis evaluation using ultrasound and choosing the most optimal VPI images in a previous ultrasound study measured the ultrasound images. One of the raters had been investigating the proposed UCA measurement for 2 years and the other rater had been learning this new measurement method for 3 months before performing data acquisition for this study. All raters performed the measurements independently, without discussing the selection of the end vertebrae levels. In addition, all the raters were blinded to the patients' details and each other's results.

This study was divided into two stages: a reliability and a validity stage (Table 1). In the reliability stage, 25 patients underwent ultrasound scans for the intra-operator test (twice by operator 1) and another 25 patients underwent scans for the inter-operator test (once by Operator 1 and once by operator 2). The repeated scans were conducted immediately after the first scan. In addition, the subjects were required to stay in the same position for both scans. For the intra- and inter-rater reliability analyses of the UCA measurements, evaluator 1 measured the UCA twice and operator 1 measured the UCA once on the same ultrasound scan, to eliminate the potential effect of different operators. The scans were conducted by operator 1. For intra- and inter-operator reliability analyses, evaluator 1 conducted UCA measurements on the three ultrasound scans, which two of them were conducted by operator 1 and one of them conducted by operator 2, to eliminate the potential effect of different raters. For the validity stage, correlations and comparison between the UCA obtained from the 50 patients in the reliability stage together with additional 114 patients with AIS and the corresponding Cobb angle measurements were investigated.

2.4. Statistical analysis

Statistical analyses were conducted using SPSS Version 20.0 for windows (IBM, SPSS Inc., USA). For the reliability stage, intra-class correlation coefficients (ICCs) were computed to investigate the reliability of the ultrasound results obtained from the same/different rater(s) and operator(s). The intra-class correlation coefficient ICC (3,1) with 95% confidence intervals (two-way mixed and absolute agreement) were used to evaluate intra-rater/operator reliabilities, whereas ICC (2,1) with 95% confidence intervals (two-way random and absolute agreement) were used to evaluate inter-rater/operator reliabilities [22]. In addition, the intra- and inter-rater/operator of the UCA were evaluated using the mean absolute difference (MAD) and standard error of measurement (SEM). The criteria for evaluating ICC values were: very reliable (0.80–1.0), moderately reliable (0.60–0.79), and questionably reliable ($\leq$0.60) [23]. Summary of the rater and operator reliability tests could be found in Table 1. For the validity stage, linear regression and correlation coefficients for main thoracic and (thoraco)lumbar curves were conducted between the ultrasound UCA and radiographic Cobb angles. Correlation coefficient of 0.25–0.50 indicates poor correlation, 0.50 to 0.75 indicates moderate to good correlation, and 0.75 to 1.00 indicates very good to excellent correlation [24]. In addition, ICC (2,1) with 95% confidence intervals (two-way random and absolute agreement), the mean absolute difference (MAD) and standard error of measurement (SEM) were used to evaluate inter-method reliabilities [22]. Furthermore, Bland–Altman plots were used to investigate the agreement between UCA and radiographic Cobb for both main thoracic and (thoraco) lumbar curves.

Table 1
Summary of data sets used in different reliability tests.

Reliability Tests	Details
Intra-rater (two-way mixed and absolute agreement)	Tests between the two UCA measurements for main thoracic and (thoraco)lumbar curves by Rater 1 on the same ultrasound image from the first scan conducted by Operator 1
Inter-rater (two-way random and absolute agreement)	Tests between the two UCA measurements for main thoracic and (thoraco)lumbar curves by Rater 1 and 2 respectively on the same ultrasound image from the first scan conducted by Operator 1
Intra-operator (two-way mixed and absolute agreement)	Tests between the two UCA measurements for main thoracic and (thoraco)lumbar curves by Rater 1 on two different ultrasound images from the first and second scans conducted by Operator 1 respectively
Inter-operator (two-way random and absolute agreement)	Tests between the two UCA measurements for main thoracic and (thoraco)lumbar curves by Rater 1 on two different ultrasound images from the first scans conducted by Operator 1 and 2 respectively
Inter-method (two-way random and absolute agreement)	Tests between the UCA measurements by Rater 1 and radiographic Cobb for main thoracic and (thoraco) lumbar

UCA: ultrasound curve angle

3. Results

A total of 50 patients with AIS, with an average of 15.2 ± 1.9 (range 11–18) years of age were involved for the reliability stage. Half of them (9 male and 16 female; mean of age: 15.4 ± 2.0 years; mean main thoracic and (thoraco)lumbar Cobb: 25.1 ± 9.6° and 24.0 ± 9.1° respectively) were involved for intra-operator and intra- and inter-rater reliability tests, whereas the other half (2 male and 23 female; mean of age: 15.0 ± 1.8 years; mean main thoracic and (thoraco)lumbar Cobb: 25.5 ± 8.8° and 27.2 ± 9.4° respectively) were involved for inter-operator reliability tests. Another 114 patients with AIS were recruited for the validity stage, combining the 50 patients involved in the reliability stage, total 164 subjects were included (33 male and 131 female subjects; 11–18 years of age, mean of 15.1 ± 1.9 years). Mean radiographic Cobb angle measured in the main thoracic and (thoraco)lumbar region of these patients were 27.2 ± 11.6° (range 8.8–59.4°) and 26.2 ± 11.4° (range 8.2–70.3°) respectively, whereas the mean ultrasound UCA measured in the main thoracic and (thoraco)lumbar region of these patients were 26.3 ± 11.4° (range 7.9–59.9°) and 24.8 ± 9.7° (range 8.0–71.7°) respectively. The average time required for UCA measurement on the ultrasound image for each scan was less than 30 s.

3.1. Reliability

All the intra- and inter-rater/operator variation and reliability for the UCA measurements of coronal spinal curvatures were summarized in Table 2. The ICC (3,1) values for intra-rater reliabilities of UCA measurements were 0.982 (95% confidence interval: 0.958–0.993) and 0.976 (95% confidence interval: 0.938–0.991) respectively for main thoracic and (thoraco)lumbar curves, with MAD ranging from 0° to 3.4° and SEM from 0.1° to 1.7° for main thoracic angles and MAD ranging from 0° to 4.0° and SEM from 0° to 2.0° for (thoraco)lumbar angles. The ICC (2,1) values for inter-rater reliabilities of UCA measurements were 0.969 (95% confidence interval: (0.926–0.987) and 0.925 (95% confidence interval: 0.813–0.971), respectively, for main thoracic and (thoraco)lumbar curves, with MAD ranging from 0° to 4.3° and SEM from 0.1° to 2.2° for main thoracic angles and MAD ranging from 0.7° to 8.3° and SEM from 0.4° to 4.1° for (thoraco)lumbar angles. The ICC (3,1) values for intra-operator reliabilities of UCA measurements were 0.973 (95% confidence interval: 0.936–0.989) and 0.975 (95% confidence interval: 0.935–0.991), respectively, for main thoracic and (thoraco)lumbar curves, with MAD ranging from 0.3° to 5.9° and SEM from 0.1° to 3.0° for main thoracic angles and MAD ranged from 0° to 4.7° and SEM from 0° to

Table 2
Intra- and inter-rater and intra- and inter-operator variation and reliability of ultrasound curve angle measurements on main thoracic and (throaco)lumbar curves.

UCA measurement	Main Thoracic Curves			(Thoraco)lumbar Curves		
	ICC (2,1)[a]/ICC (3,1)[b] (95%CI)	MAD(°)	SEM(°)	ICC (2,1)[a]/ICC (3,1)[b] (95%CI)	MAD(°)	SEM(°)
Intra-rater	0.982(0.958–0.993)[b]	1.4 (0.0–3.4)	0.8 (0.1–1.7)	0.976 (0.938–0.991)	1.3 (0.0–4.0)	0.9 (0.0–2.0)
Inter-rater	0.969(0.926–0.987)[a]	1.7 (0.0–4.3)	1.0 (0.1–2.2)	0.925 (0.813–0.971)	3.5 (0.7–8.3)	1.7 (0.4–4.1)
Intra-operator	0.973(0.936–0.989)[b]	1.9 (0.3–5.9)	0.9 (0.1–3.0)	0.975 (0.935–0.991)	1.8 (0.0–4.7)	0.9 (0.0–2.4)
Inter-operator	0.984(0.955–0.994)[a]	1.0 (0.0–3.2)	0.6 (0.0–1.6)	0.963 (0.880–0.986)	2.0 (0.0–4.0)	1.0 (0.0–2.0)

CI: confidence interval; ICC: Intraclass correlation coefficient; MAD: mean absolute difference; SEM: standard error of measurement; UCA: ultrasound curve angle
[a] ICC computed using two-way random and absolute agreement
[b] ICC computed using two-way mixed and absolute agreement;

2.4° for (thoraco)lumbar angles. The ICC (2,1) values for inter-operator reliabilities of UCA measurements were 0.984 (95% confidence interval: 0.955–0.994) and 0.963 (95% confidence interval: 0.880–0.986), respectively, for main thoracic and (thoraco)lumbar curves, with MAD ranging from 0° to 3.2° and SEM from 0° to 1.6° for main thoracic angles and MAD ranged from 0° to 4.0° and SEM from 0° to 2.0° for (thoraco) lumbar angles. The above results demonstrated that the both the intra- and inter-reliabilities of the UCA, in terms of rater and scanning operator, were high.

3.2. Validity

Main thoracic and (thoraco)lumbar UCA showed very good linear correlations with the radiographic Cobb angles for main thoracic (R^2=0.884) and (thoraco)lumbar curves (R^2=0.893) (Fig. 6). If we counted all the angles together, the R^2 value between the two modalities was 0.888. The scaling factors between UCA and Cobb angle obtained from the linear equation were 1.024 and 1.048 for the main thoracic and (thoraco)lumbar curves, respectively, and it was 1.035 if we combined all the together. The inter-method variations between Cobb angles and UCA measurements were summarized in Table 3. The ICC (2,1) values for inter-method variations were 0.945 (95% confidence interval: 0.920–0.961) and 0.933 (95% confidence interval: 0.883–0.959), respectively, for main thoracic and (thoraco)lumbar curves, with MAD ranging from 0° to 9.9° and SEM from 0° to 5.0° for main thoracic angles and MAD ranging from 0° to 11.9° and SEM from 0° to 5.9° for (thoraco) lumbar angles. The overall MADs for main thoracic and (thoraco)lumbar angles were 3.0° and 2.8° respectively. Eighty-three percent (106 out of

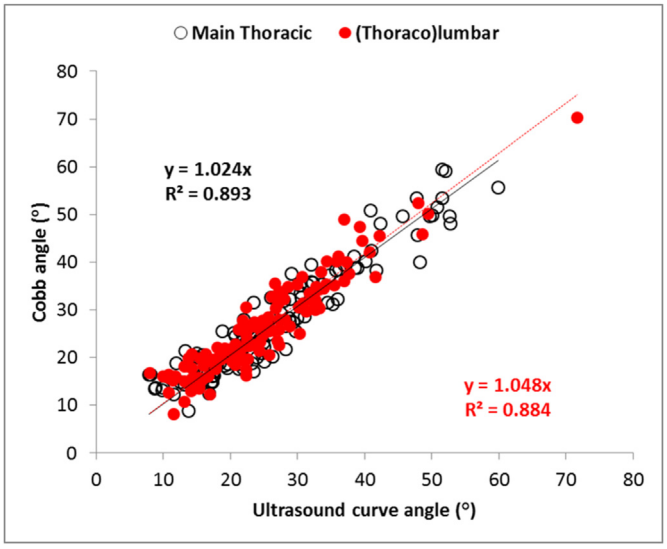

Figure 6. Correlations (R^2) and regression equations between the radiographic Cobb angles and ultrasound curve angle are shown for the main thoracic (black) and the (thoraco)lumbar (red) curves.

Table 3
Inter-method variations and reliability between Cobb angles and ultrasound curve angle measurements on main thoracic and (throaco)lumbar curves.

Curves	Comparison between Cobb and ultrasound curve angle			
	ICC (2,1) (95% CI)	MAD(°)	SEM(°)	% within 5° difference
Main thoracic	0.945 (0.920–0.961)	3.0 (0.0–9.9)	1.5 (0.0–5.0)	83
(Thoraco) lumbar	0.933 (0.883–0.959)	2.8 (0.0–11.9)	1.4 (0.0–5.9)	83

CI: confidence interval; ICC: Intraclass correlation coefficient; MAD: mean absolute difference; SEM: standard error of measurement

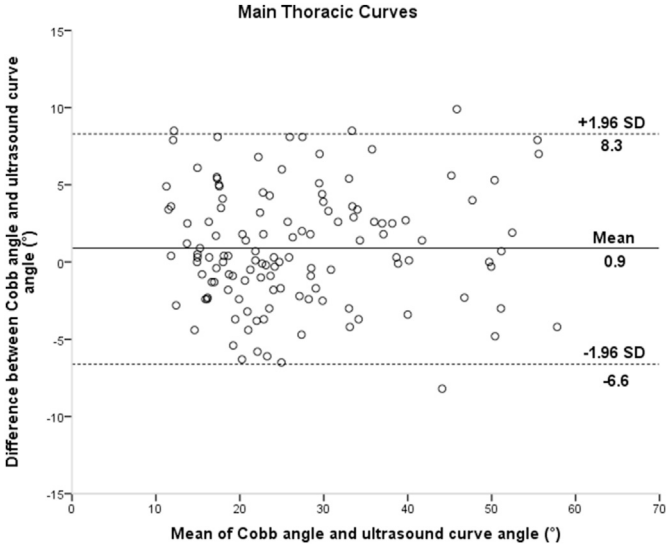

Figure 7. Bland–Altman plots which demonstrates the differences between the Cobb angles and the coronal ultrasound angles for main thoracic curves. The central line represents the bias and the dotted lines represent the 95% limits of agreement.

128 curves) of the main thoracic UCA and eighty-three percent (106 out of 127 curves) of (thoraco)lumbar UCA were within 5° difference compared with radiographic Cobb. Figs. 7 and 8 demonstrated that a good agreement between UCA and radiographic Cobb angle measurement for coronal curvatures. According to Bland–Altman plots (Figs. 7 and 8), the bias, 95% upper and lower limits of agreements were 0.9°, 8.3° and −6.6° for main thoracic curves and 1.8°, 8.7° and −5.1° for (thoraco)lumbar curves, respectively.

4. Discussion

Conduction 3D ultrasound imaging of the back of patients with AIS could only allow viewing the posterior structure of the spine. The anterior features such as the vertebral bodies and intervertebral disc could

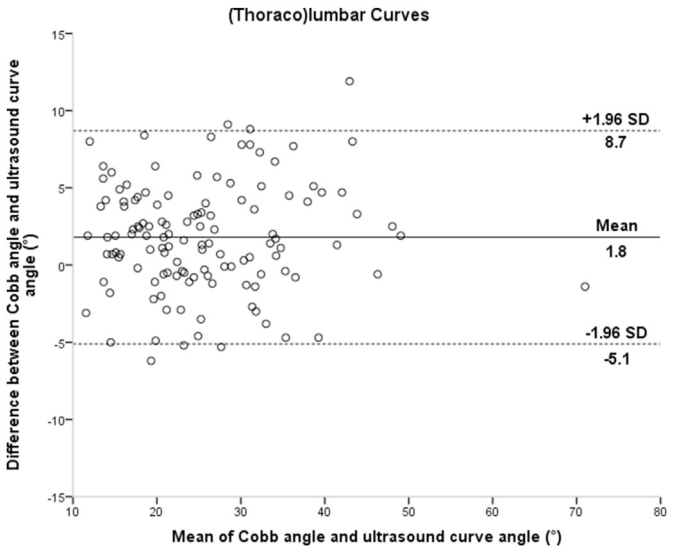

Figure 8. Bland–Altman plots which demonstrates the differences between the Cobb angles and the coronal ultrasound angles for (thoraco)lumbar curves. The central line represents the bias and the dotted lines represent the 95% limits of agreement.

not be seen because ultrasound could not penetrate through bones. In addition, information such as pelvic parameters, leg discrepancies and rib cage disorder could not be reviewed from a 3D ultrasound scan. Hence, ultrasound could be treated as a non-invasive and non-ionizing tool to provide supplementary data for traditional radiographic approach and serve as a tool for scoliosis screening and monitoring curve progression by providing more frequent scanning for patients with mild and moderate AIS, but not replacing radiograph.

For radiographic Cobb measurements, the ICC values obtained on patients with AIS, with similar Cobb range compared to this study, ranged from 0.87 to 0.97 for intra-rater repeatability and from 0.87 to 0.98 for inter-rater repeatability in previous studies [25,26], whereas for ultrasound SPA measurements conducted on ultrasound images generated from the 3D ultrasound imaging system, the ICC values obtained ranged from 0.87 to 0.97 for intra-rater repeatability and from 0.84 to 0.99 for inter-rater repeatability, similar to that obtained from the SonixTABLET ultrasound imaging system using COL method [14]. In addition, the intra- and inter-operator reproducibility for ultrasound SPA measurements obtained in two previous ultrasound studies, in which the coronal images were generated using the VPI method based on back surface, ranged from 0.84 to 0.97 [10,11]. In this study, the intra- and inter-reliabilities for raters (repeatability) and operators (reproducibility) using the UCA measurements were demonstrated to be as high as all the above studies, indicating that the ultrasound scanning and UCA measurements were repeatable and reproducible when measuring coronal curvatures for patients with AIS in main thoracic and (thoraco)lumbar region. Very good linear correlations ($R^2 \geq 0.884$), with range of ICC values from 0.883 to 0.961 and MAD with no more than 3° were demonstrated between UCA and radiographic Cobb angles. In addition, 83% of the curves were found to be within 5° difference comparing between the UCA and Cobb angles. Similar results were reported earlier using different 3D ultrasound imaging system for scoliosis assessment applied on either spine phantoms [14,21,27,28] or patients with AIS [10,11,13,15,16,25]. The reliability and validity of using transverse processes and superior articular processes on ultrasound imaging for coronal measurements were demonstrated in previous phantom studies [27,28], and the usage of both landmarks was found to yield better correlation and agreement between the ultrasound and radiographic Cobb angles than using transverse processes alone. Better correlations between ultrasound and Cobb angles using linear regression were achieved in two previous studies using SPA and COL method respectively than this study [11,16], but the sample sizes of those studies were much smaller ($N \geq 33$). There were very slight differences between the linear regression and correlations of the UCA and Cobb angle. This could possible due to thicker muscles and fat tissues and the absence of ribs for reference in the (thoraco)lumbar region, though these factors did not have a striking impact on the reliability and validity. In addition, the overall MAD and SEM between UCA and radiographic Cobb measurements were no larger than 3.0° and 1.5° respectively for both types of curves. These results showed that the ultrasound angle obtained in this study had a close-to-one relationship with coronal Cobb and can reflect the curve severity of the patients when compared to Cobb angle.

Yet the findings in this study were different from that obtained from previous study using the same ultrasound imaging system, where the scaling factors between SPA and Cobb angle obtained from the linear equation were 1.200 and 1.154 for main thoracic and (thoraco)lumbar curves respectively [10]. The major reasons that cause such discrepancies are: 1) Spinous processes used for previous studies were anatomical features relatively posterior and subjected to deformation in patients with severe scoliosis [29]; 2) measurement method of UCA is more similar to traditional Cobb method when compared with that of SPA. Scaling factors of the linear equations between transverse processes angle and Cobb angle obtained in Brink et al.'s study were different from those in this study, where the factors were 1.297 and 1.163 for thoracic and (thoraco)lumbar regions, respectively [11]. The difference was possibly caused by the improvable lines placement on the coronal ultrasound images using the back surface based VPI due to the vague definition of the bilateral vertebrae features, which justified the need of alternative VPI and measurement methods in this study. Different from the previous study [10,11], instead of using back surfaces of the patients as reference to generate coronal images, a different VPI method based on the depth of vertebrae bony structure under the skin was applied to generate the coronal images in this study. This is because the distances between the vertebrae features used for UCA measurement and skin surface vary at different vertebrae levels [18,30], thus coronal images generated using vertebra-depth-dependent VPI would allow raters to have a better visualization of the bilateral vertebrae features such as transverse processes, bilateral laminae and articular processes ultimately facilitates the line placement for the UCA measurement. In future studies, a reference table which facilitates reconstruction of vertebra-depth-dependent VPI could be formulated using computed tomography, in order to generate the most optimal coronal images for UCA measurement.

Correlation between ultrasound and X-ray results was found to be unsatisfactory for curves with apices above T6 in a previous study due to the design of the ultrasound probe [12], thus only main thoracic and (thoraco)lumbar curves were analyzed in this study. A special scanning technique or flexible ultrasound transducer could be implemented to tackle the scanning of proximal curves in future study. In addition, different features were used for UCA measurement in the main thoracic and (thoraco)lumbar region. In the thoracic region, transverse processes were selected for measurement because they appeared to be smaller and more observable in the ultrasound images [31], therefore the line placement could be conducted more precisely if more lateral elements were involved in measurement. However, since transverse processes of the vertebrae in the lumbar region were further apart and more anteriorly located compared to those in the thoracic region, which was beyond the width of the ultrasound probe in most of the cases, the bilateral superior articular processes shadows were selected for angle measurement in the lumbar region.

The alternative VPI profile was obtained based on the average skin-to-laminae distances of 40 patients with AIS of different curves severity, thus the projected coronal images may not be the most optimal for UCA evaluation. In future study, the reliability of the selection of the VPI images and the effect of adopting different VPI method on UCA measurement should be investigated. An additional research direction is to use deep learning method to achieve automatic selection of the most

optimized image for measurement [32]. Not all vertebrae features were clearly visible in some coronal ultrasound images, which induced difficulty in identifying these features and drawing lines on them, ultimately affecting the accuracy of UCA measurement. There are several reasons which caused such problem. First, poor contact between the ultrasound and the patients' back, such as the presence of narrow gap between the scapula, causes darkened area of some images if not enough coupling gel was used during scanning. Second, the vertebrae features which were too far away from the skin surface would cause extra attenuation by the tissues to ultrasound and reduced penetration and image quality. This could be subjected to the sagittal profile, muscular thickness and fat deposit of the patients' back. Third, the presence of vertebral rotation, especially in the lumbar region, would greatly affect the coverage of all bilateral vertebrae features and the entire coronal spinal profile in a single ultrasound layer after volume projection as one side of the vertebrae structures were further away from the skin surface. The system used in this study adopted a linear ultrasound probe with frequency of 7.5 MHz, which provided very good resolution. The system can be improved by including a probe with lower ultrasound frequency, such as 3.5 or 5 MHz to facilitate achieving better penetration with image resolutions sacrificed slightly. To obtain more lateral features, such as transverse processes in the lumbar region, an ultrasound probe with a curved surface or a fan scanning profile can be used in future studies. Moreover, it should be noted that the 3D information, such as apex rotation, was lost during VPI coronal projection, it is also essential to validate ultrasound measurements in 3D against a true 3D radiographic assessment to fully utilize the information contained in 3D ultrasound images. In addition, further studies should be carried out to investigate the primary cause which leads to measurement error for the ultrasound images, such as utilizing the Generalisabilty theory to study the effect of remeasuring or reacquiring an image and investigating the effect of the degree of blindness such as choice of image layers and the selection of upper and lower endplate vertebrae on angle analysis. The Cobb angle involved in this study was relatively small, the reasons behind this observation were: 1) Some of the patients with large curves were receiving brace treatments to control curve progression; 2) Ultrasound images acquired from three patients with Cobb larger than 50° were too poor to be analyzed and were thus not included in the analysis, due to the narrow scapula and presence of vertebrae rotation which possibly reflect ultrasound signal away from the transducer, leading to unsatisfying image quality. Furthermore, the arms position of the patients with AIS was different during ultrasound and X-ray evaluation, which could also cause the angle discrepancies between the radiographic Cobb and ultrasound curve angle.

The specificity and sensitivity for detection of curve progression and judgment for assigning treatments using different coronal ultrasound angles by the 3D ultrasound imaging should be investigated in future studies. It would also be essential to study the cut-off angle of UCA to define curve progression. In addition, the 3D ultrasound imaging system had also been demonstrated to provide dynamic change of the coronal curvature assessment during different postures such as lateral bending [33] and forward bending [34], UCA could also be used to evaluate the change in future study.

5. Conclusions

UCA appeared to be a reliable and valid parameter for evaluating coronal curvatures of scoliotic spine of AIS, without overall clinical differences when compared to radiographic Cobb angles. Judging from the promising results from the ultrasound measurement of this study, patients with AIS with different severity of curves can be evaluated and monitored by ultrasound imaging, reducing the usage of radiation during follow-ups. This method could also be used for scoliosis screening.

Authorship

Conception and design of study: T.T.Y. Lee, R.M. Castelein, J.C.Y. Cheng, Y.P. Zheng. Acquisition of data: T.T.Y. Lee, K.K.L. Lai, T.P. Lam. analysis and/or interpretation of data: T.T.Y.Lee. Drafting the manuscript: T.T.Y. Lee, K.K.L. Lai. Revising the manuscript critically for important intellectual content: R.M. Castelein, J.C.Y. Cheng, T.P. Lam, Y.P. Zheng. Approval of the version of the manuscript to be published (the names of all authors must be listed): T.T.Y. Lee, K.K.L. Lai, J.C.Y. Cheng, R.M. Castelein, T.P. Lam, Y.P.Zheng.

Funding Disclosure(s) statement

This project was supported by Hong Kong Research Grant Council Research Impact Fund (R5017-18). Y.P. Zheng reports his role as a consultant to Telefield Medical Imaging Limited for the development of Scolioscan, outside the submitted work and he is the inventor of a number of patents related to 3D ultrasound imaging for scoliosis, which has been licensed to Telefield Medical Imaging Limited through Hong Kong Polytechnic University. In addition, R.M. Castelein received funding from Stryker Spine Research Grant.

Funding/support statement

The work was supported by the funding from Hong Kong Research Grant Council Research Impact Fund (R5017-18); and the Stryker Spine Research Grant.

Declaration of competing interest

The corresponding author reported his role as a consultant to a company for the development of the 3D ultrasound imaging system and was the inventor of a number of patents related to 3D ultrasound imaging for scoliosis, licensed to the corresponding company. All the other author(s) have no conflicts of interest relevant to this article.

Acknowledgements

All persons who have made substantial contributions to the work reported in the manuscript (e.g., technical help, writing and editing assistance, general support), but who do not meet the criteria for authorship, are named in the Acknowledgements and have given us their written permission to be named. If we have not included an Acknowledgements, then that indicates that we have not received substantial contributions from non-authors.

References

[1] Cheng JC, Castelein RM, Chu WCC, Danielsson AJ, Dobbs MB, Grivas TB, et al. Adolescent idiopathic scoliosis. Nat Rev Dis Primer 2015;1:15068.
[2] Simony A, Hansen EJ, Christensen SB, Carreon LY, Andersen MO. Incidence of cancer in adolescent idiopathic scoliosis patients treated 25 years previously. Eur Spine J 2016;25(10):3366–70.
[3] Deschênes S, Charron G, Beaudoin G, Labelle H, Dubois J, Miron MC, et al. Diagnostic imaging of spinal deformities reducing patients radiation dose with a new slot-scanning X-ray imager. Spine 2010;35:989–94.
[4] Mitulescu A, Skalli W, Mitton D, De Guise JA. Three-dimensional surface rendering reconstruction of scoliotic vertebrae using a non stereo-corresponding points technique. Eur Spine J 2002;11:344–52.
[5] Oakley PA, Ehsani NN, Harrison DE. The scoliosis quandary: are radiation exposures from repeated X-rays harmful? Dose Response 2019;17(2). 1559325819852810.
[6] Presciutti SM, Karukanda T, Lee M. Management decisions for adolescent idiopathic scoliosis significantly affects patient radiation exposure. Spine J 2014;14(9): 1984–90.
[7] Faria R, McKenna C, Wade R, Yang H, Woolacott N, Sculpher M. The EOS 2D/3D X-ray imaging system: a cost-effectiveness analysis quantifying the health benefits from reduced radiation exposure. Eur J Radiol 2013;82(8):e342–9.
[8] Navarro IJRL, Rosa BND, Candotti CT. Anatomical reference marks, evaluation parameters and reproducibility of surface topography for evaluating the adolescent idiopathic scoliosis: a systematic review with meta-analysis. Gait Posture 2019;69: 112–20.
[9] Suzuki S, Yamamuro T, Shikata J, Shimizu K, Iida H. Ultrasound measurement of vertebral rotation in idiopathic scoliosis. J Bone Joint Surg Br 1989;71(2):252–5.

[10] Zheng YP, Lee TTY, Lai KK, Yip BH, Zhou GQ, Jiang WW, et al. A reliability and validity study for Scolioscan: a radiation-free scoliosis assessment system using 3D ultrasound imaging. Scoliosis Spinal Disord 2016;11:13.
[11] Brink RC, Wijdicks SPJ, Tromp IN, Schlösser TPC, Kruyt MC, Beek FJA, et al. A reliability and validity study for different coronal angles using ultrasound imaging in adolescent idiopathic scoliosis. Spine J 2018;18(6):979–85.
[12] Wong YS, Lai KK, Zheng YP, Wong LL, Ng BK, Hung AL, et al. Is radiation-free ultrasound accurate for quantitative assessment of spinal deformity in idiopathic scoliosis (IS): a detailed analysis with EOS radiography on 952 patients. Ultrasound Med Biol 2019;45(11):2866–77.
[13] Li M, Cheng J, Ying M, Ng B, Zheng Y, Lam T, et al. Could clinical US improve the fitting of spinal orthosis for the patients with AIS? Eur Spine J 2012;21(10):1926–35.
[14] Chen W, Lou EH, Zhang PQ, Le LH, Hill D. Reliability of assessing the coronal curvature of children with scoliosis by using US images. J Child Orthop 2013;7(6):521–9.
[15] Young M, Hill DL, Zheng R, Lou E. Reliability and accuracy of US measurements with and without the aid of previous radiographs in adolescent idiopathic scoliosis (AIS). Eur Spine J 2015;24(7):1427–33.
[16] Wang Q, Li M, Lou EH, Wong MS. Reliability and validity study of clinical ultrasound imaging on lateral curvature of adolescent idiopathic scoliosis. PloS One 2015;10(8):e0135264.
[17] Lee TTY, Cheung JCW, Law SY, To MKT, Cheung JPY, Zheng YP. Analysis of sagittal profile of spine using 3D ultrasound imaging: a phantom study and preliminary subject test. CMBBE: Imaging and Visualization 2019. https://doi.org/10.1080/21681163.2019.1566025.
[18] Lee TTY, Jiang WW, Cheng CLK, Lai KKL, Begovic H, To MKT, et al. A novel method to measure the sagittal curvature in spinal deformities: the reliability and feasibility of 3-D ultrasound imaging. Ultrasound Med Biol 2019b;45(10):2725–35.
[19] Ungi T, King F, Kempston M, Keri Z, Lasso A, Mousavi P, et al. Spinal curvature measurement by tracked ultrasound snapshots. Ultrasound Med Biol 2014;40(2):447–54.
[20] Glaser DA, Doan J, Newton PO. Comparison of 3-dimensional spinal reconstruction accuracy: biplanar radiographs with EOS versus computed tomography. Spine 2012;37(16):1391–7.
[21] Cheung CW, Zhou GQ, Law SY, Mak TM, Lai KL, Zheng YP. Ultrasound volume projection imaging for assessment of scoliosis. IEEE Trans Med Imag 2015;34(8):1760–8.
[22] Shrout PE, Fleiss JL. Intraclass correlations: uses in assessing rater reliability. Psychol Bull 1979;86(2):420–8.
[23] Currier DP. Elements of research in physical therapy. 3rd ed. Baltimore: Williams & Wilkins; 1984. p. 162.
[24] Dawson B, Trapp RG. Research questions about relationships among variables. In: Basic and Clinical Biostatistics. 4th edn. Lange Medical Books/McGraw-Hill; 2004. p. 190–220.
[25] Gstoettner M, Sekyra K, Walochnik N, Winter P, Wachter R, Bach CM. Inter- and intraobserver reliability assessment of the Cobb angle: manual versus digital measurement tools. Eur Spine J 2007;16(10):1587–92.
[26] Mok JM, Berven SH, Diab M, Hackbarth M, Hu SS, Deviren V. Comparison of observer variation in conventional and three digital radiographic methods used in the evaluation of patients with adolescent idiopathic scoliosis. Spine 2008;33(6):681–6.
[27] Cheung CW, Law SY, Zheng YP. Development of 3-D US system for assessment of adolescent idiopathic scoliosis (AIS): and system validation. Conf Proc IEEE Eng Med Biol Soc 2013:6474–7.
[28] Cheung CWJ, Zhou GQ, Law SY, Lai KL, Jiang WW, Zheng YP. Freehand three-dimensional ultrasound system for assessment of scoliosis. JOT 2015;3(3):123–33.
[29] Kotwicki T, Napiontek M. Intravertebral deformation in idiopathic scoliosis: a transverse plane computer tomographic study. J Pediatr Orthop 2008;28(2):225–9.
[30] Avramescu S, Arzola C, Tharmaratnam U, Chin KJ, Balki M. Sonoanatomy of the thoracic spine in adult volunteers. Reg Anesth Pain Med 2012;37(3):349–53.
[31] Ferràs-Tarragó J, Valencia JMM, Belmar PR, Vergara SP, Gómez PJ, Hermida JLB, et al. Cobb angle measurement with a conventional convex echography probe and a smartphone. Eur Spine J 2019;28(9):1955–61.
[32] Lyu J, Ling SH, Banerjee S, Zheng JY, Lai KL, Yang D, et al. Ultrasound volume projection image quality selection by ranking from convolutional RankNet. Comput Med Imag Graph 2021;89:101847.
[33] He C, To MK, Cheung JP, Cheung KM, Chan CK, Jiang WW, et al. An effective assessment method of spinal flexibility to predict the initial in-orthosis correction on the patients with adolescent idiopathic scoliosis (AIS). PloS One 2017;12(12):e0190141.
[34] Jiang WW, Cheng CLK, Cheung JPY, Samartzis D, Lai KKL, To MKT, et al. Patterns of coronal curve changes in forward bending posture: a 3D ultrasound study of adolescent idiopathic scoliosis patients. Eur Spine J 2018;27(9):2139–47.